

# A Sensor for Parts Inspection

S. M. Tam and K. C. Cheung  
Department of Mechanical Engineering  
The University of Hong Kong  
Pokfulam Road, Hong Kong

**Abstract**—This paper describes the development of a sensor which performs parts inspection by measuring the inertial properties of the part. The sensor comprises a platform supported on a column which is fixed to a rigid base. The part under inspection is attached to the platform to form a single body. By measuring the static deflections of the column and the natural frequencies of vibration of the system, it is possible to determine the mass and the spatial location of the centre of mass of the part. The information obtained is then used to distinguish defective parts from good ones.

## 1. Introduction

Inspection is usually required to ensure that a part is machined according to its specification. It often involves measuring various attributes of the part under inspection and comparing the measured values against those specified. The attributes being measured may include the size, shape, mass, locations and sizes of drilled holes and locations and sizes of milled slots of the part.

Human inspection, which measures those attributes manually using vernier callipers, micrometers, balances and gauges, is ineffective and expensive. In order to increase the efficiency of quality inspection, automated inspection systems were introduced. Vision system is commonly used for the automatic inspection of parts[1].

In a vision system, video cameras are used to capture, from one or more angles, the images of the part under inspection and a computer used for signal analysis. The analysis was done by comparing the images of the part with those of a good part. Therefore, a camera with higher resolution will give a more accurate result. Although high resolution makes the system accurate, a large volume of image data needs to be handled, resulting in long cycle times. Moreover, the quality of the captured images are seriously affected by working conditions such as poor lighting and smoky environment. Also, internal defects such as presence of internal void cannot be detected by vision system.

To overcome the deficiencies of vision-based inspection systems, it is desirable to have a sensor which inspects parts by measuring properties of the part other than its appearance.

The fundamental difference between a good part and a defective one lies with their masses and locations of centres of mass. Generally, a defective part will have a different

mass as well as a different location of centre of mass compared with a good part, irrespective of the defect.

This paper reports on the development of a sensor which measures the mass and the location of the centre of mass of a given part. Figure 1 shows a schematic view of the proposed sensor with the associated coordinate system.

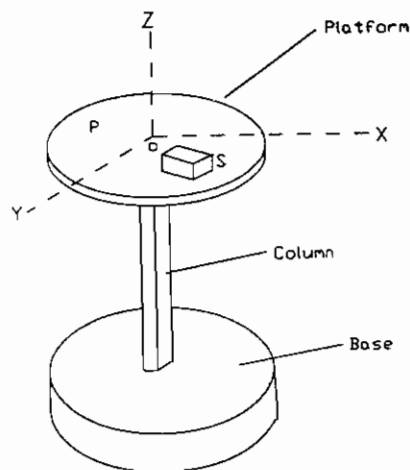


Figure 1. Schematic view of sensor

## Nomenclature

$L$	length of column
$X_g, Y_g, Z_g$	coordinates of the centre of mass
$I_{XX}, I_{YY}$	second moment of area of the cross-section of the column about the x- and y-axes respectively
$E$	Young's modulus of the column
$\theta_{XS}, \theta_{YS}$	deflections of column in the x and y axes respectively
$I_{MX}, I_{MY}$	moments of inertia of the test piece about the x and y axes respectively
$m$	mass of test piece
$m_p$	mass of platform
$m_c$	mass of column
$f_x, f_y$	natural frequencies of the system when vibrating within the x-z and y-z planes
$I_{CX}, I_{CY}$	moments of inertia of the sensor body about the x and y axes respectively
$K_x, K_y$	bending stiffness of column at x and y axes respectively
$K_{XX}$	linear stiffness of column at the x axis

## 2. Operation

The part S is placed onto platform P and held firmly by a magnetic sheet. The purpose is to ensure that S and P act like a single rigid body. This does not limit the use of the sensor to ferrous objects because non-ferrous objects can be fixed onto the platform by means of jig and jaws. The platform is rigid while the column is elastic. Three sets of strain gauges mounted on the column as shown in Figure 2 measure the static deflections of the column. The system is then set into free vibration by an impact from a solenoid actuated bolt. The free vibration of the sensor body with the object is measured by the strain gauges. An I/O interface circuit together with a microcomputer determine the frequencies of vibration. The microcomputer with corresponding software then uses the static deflections and the natural frequencies of vibration to calculate the mass and the spatial location of the centre of mass of an object placed on the platform.

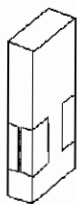


Figure 2. Strain gauges mounted on the column

## 3. Theory

This section outlines the methods for obtaining mass and coordinates of the centre of mass ( $X_g$ ,  $Y_g$ ,  $Z_g$ ) of the object. The microcomputer then uses this data to distinguish defective parts from good ones.

### 3.1 Mathematical Model

#### Static deflections

When an object is placed on the platform of the sensor, the static deflections of the column,  $\theta_{xs}$  and  $\theta_{ys}$  are given by the static equilibrium equation below.

$$\begin{pmatrix} K_x \\ K_y \end{pmatrix} \cdot \begin{pmatrix} \theta_{xs} \\ \theta_{ys} \end{pmatrix} = \begin{pmatrix} -m g X_g \\ -m g Y_g \end{pmatrix} \quad (1)$$

where  $K_x$  and  $K_y$  are the bending stiffness of the column in the x and y axes respectively.

$$K_x = \frac{3 E I_{xx}}{L^2} \quad K_y = \frac{3 E I_{yy}}{L^2}$$

Equation (1) can be re-arranged as

$$\begin{pmatrix} \theta_{xs} \\ \theta_{ys} \end{pmatrix} = \begin{pmatrix} -m g X_g \\ -m g Y_g \end{pmatrix} \cdot \begin{pmatrix} K_x \\ K_y \end{pmatrix}^{-1} \quad (2)$$

The deflections,  $\theta_{xs}$  and  $\theta_{ys}$  are measured by strain gauges mounted on the column as shown in Figure 2.

The voltage outputs of the strain gauge bridges are proportional to the static deflections and can be expressed as

$$V_x = S_x \cdot m \cdot X_g \quad (3)$$

$$V_y = S_y \cdot m \cdot Y_g \quad (4)$$

$S_x$  and  $S_y$  are the constants of proportionality. The mass of the part,  $m$ , can then be expressed as:

$$m = \frac{V_x}{S_x \cdot X_g} = \frac{V_y}{S_y \cdot Y_g}$$

Let  $C_x = \frac{V_x}{S_x}$  and  $C_y = \frac{V_y}{S_y}$  then the equations can be rearranged as:

$$m = \frac{C_x}{X_g} = \frac{C_y}{Y_g} \quad (5)$$

and

$$Y_g = \frac{C_y}{C_x} \cdot X_g \quad (6)$$

#### Natural frequencies of vibration

The frequency equations of the sensor are derived using the Energy Method which is suitable for analyzing systems under free-vibration.

The Kinetic Energy ( $T_x$ ) of the column when vibrating within the x-z plane is given by [2] as

$$T_x = \frac{1}{2} I_{cx} \dot{\theta}_{xs}^2 + \frac{1}{2} (I_{mx} + m X_g^2) \dot{\theta}_{xs}^2 + \frac{1}{2} m (L + Z_g)^2 \dot{\theta}_{xs}^2$$

The Potential Energy ( $P_x$ ) stored in the column is given by [2] as

$$P_x = \frac{1}{2} K_{xx} [(L + Z_g) \theta_{xs}]^2$$

where  $K_{xx} \approx \frac{3 E I_{xx}}{(L + Z_g)^3}$  is the linear stiffness of the column.

Therefore,

$$P_x = \frac{1}{2} \left[ \frac{3EI_{xx}}{(L+Z_g)} \right] \cdot \theta_{xs}^2$$

Free vibration involves the cyclic interchange of kinetic energy and potential energy. For free vibration with negligible damping, it can be assumed that no energy is dissipated. Therefore, the sum of kinetic energy and potential energy remains constant.

$$T_x + P_x = \text{constant}$$

Therefore, 
$$\frac{d}{dt}(T_x + P_x) = 0$$

Substituting yields

$$\left[ I_{cx} + I_{mx} + mX_g^2 + m(L+Z_g)^2 \right] \ddot{\theta}_{xs} + \frac{3EI_{xx}}{(L+Z_g)} \dot{\theta}_{xs} \theta_{xs} = 0$$

The above equation can be expressed as :

$$I \cdot \ddot{\theta}_{xs} + K \cdot \theta_{xs} = 0 \quad (7)$$

where

$$I = \left[ I_{cx} + I_{mx} + mX_g^2 + m(L+Z_g)^2 \right]$$

and

$$K \approx \frac{3EI_{xx}}{(L+Z_g)}$$

Equation (7) is a typical undamped free-vibration equation with natural frequency

$$f_y = \frac{1}{2\pi} \sqrt{\frac{K}{I}}$$

Substituting K and I gives

$$f_y = \frac{1}{2\pi} \sqrt{\frac{3EI_{xx}}{m(L+Z_g)^3 + (I_{cx} + I_{mx} + mX_g^2)(L+Z_g)}}$$

where  $I_{cx} \cong I_{cy} \cong \left( \frac{33}{140} m_c + m_p \right) \cdot L^2$  [2]

Normally,  $I_{mx}$  is small compared with other terms. Therefore, it can be ignored in the calculation. Thus, the equation can be revised as follows :

$$f_y = \frac{1}{2\pi} \sqrt{\frac{3EI_{xx}}{m(L+Z_g)^3 + \left[ \left( \frac{33}{140} m_c + m_p \right) L^2 + mX_g^2 \right] (L+Z_g)}} \quad (8)$$

Similarly,  $f_x$  can be expressed as :

$$f_x = \frac{1}{2\pi} \sqrt{\frac{3EI_{yy}}{m(L+Z_g)^3 + \left[ \left( \frac{33}{140} m_c + m_p \right) L^2 + mX_g^2 \right] (L+Z_g)}} \quad (9)$$

$f_y$  and  $f_x$  are the measured natural frequencies of vibrations of the system.

### 3.2 Solving for $m$ , $X_g$ , $Y_g$ and $Z_g$

Substituting equations (5) and (6) into equations (8) and (9) gives two non-linear equations with two unknowns,  $X_g$  and  $Z_g$ .

$$f_y = \frac{1}{2\pi} \sqrt{\frac{3EI_{xx}X_g}{C_x(L+Z_g)^3 + \left[ \left( \frac{33}{140} m_c + m_p \right) L^2 X_g + C_x X_g^2 \right] (L+Z_g)}} \quad (10)$$

$$f_x = \frac{1}{2\pi} \sqrt{\frac{3EI_{yy}X_g}{C_x(L+Z_g)^3 + \left[ \left( \frac{33}{140} m_c + m_p \right) L^2 X_g + \frac{C_y^2}{C_x} X_g^2 \right] (L+Z_g)}} \quad (11)$$

Equations (10) and (11) have no analytical solution and therefore have to be solved numerically.

Newton's method [3] is then used to solve the above non-linear equations.

Firstly, the equations are rearranged as :

$$\frac{1}{2\pi} \sqrt{\frac{3EI_{xx}X_g}{C_x(L+Z_g)^3 + \left[ \left( \frac{33}{140} m_c + m_p \right) L^2 X_g + C_x X_g^2 \right] (L+Z_g)}} - f_y = 0 \quad (12)$$

$$\frac{1}{2\pi} \sqrt{\frac{3EI_{yy}X_g}{C_x(L+Z_g)^3 + \left[ \left( \frac{33}{140} m_c + m_p \right) L^2 X_g + \frac{C_y^2}{C_x} X_g^2 \right] (L+Z_g)}} - f_x = 0 \quad (13)$$

Let

$$f(X_g, Z_g) = \frac{1}{2\pi} \sqrt{\frac{3EI_{xx}X_g}{C_x(L+Z_g)^3 + \left[ \left( \frac{33}{140} m_c + m_p \right) L^2 X_g + C_x X_g^2 \right] (L+Z_g)}} - f_y$$

$$g(X_s, Z_s) = \frac{1}{2\pi} \sqrt{\frac{3EI_r X_s}{C_x(L+Z_s)^3 + \left[\left(\frac{33}{140}m_c + m_s\right)L^2 X_s + \frac{C_x^2}{C_x} X_s^2\right](L+Z_s)}} - f_x$$

$f(X_g, Z_g)$  and  $g(X_g, Z_g)$  can be assumed to have at least continuous first partial derivatives.

The objective is to search for a solution for the following simultaneous equations

$$\begin{aligned} f(X_g, Z_g) &= 0 \\ g(X_g, Z_g) &= 0 \end{aligned}$$

The desired solution is denoted by  $S = (s, t)^T$ . Let  $X^{(0)} = (X_g^{(0)}, Z_g^{(0)})^T$  be an initial approximation of the desired solution  $S = (s, t)^T$ . The k-th step substitution can be expressed as :

$$\begin{aligned} s &= X_g^{(K)} + \xi^{(K)} \\ t &= Z_g^{(K)} + \eta^{(K)} \end{aligned}$$

where the (small) correction terms  $\xi^{(K)}$  and  $\eta^{(K)}$  serve to linearise the given equations as shown below.

$$f(X_g^{(K)} + \xi^{(K)}, Z_g^{(K)} + \eta^{(K)}) \approx f(X_g^{(K)}, Z_g^{(K)}) + \xi^{(K)} f_{X_g} + \eta^{(K)} f_{Z_g}$$

$$g(X_g^{(K)} + \xi^{(K)}, Z_g^{(K)} + \eta^{(K)}) \approx g(X_g^{(K)}, Z_g^{(K)}) + \xi^{(K)} g_{X_g} + \eta^{(K)} g_{Z_g}$$

where  $f_{X_g}$ ,  $f_{Z_g}$ ,  $g_{X_g}$  and  $g_{Z_g}$  are the first partial derivatives of  $f(X_g, Z_g)$  and  $g(X_g, Z_g)$ .

when  $X_g$  and  $Z_g$  are equal to the desired solutions  $s$  and  $t$

$$f(X_g^{(K)} + \xi^{(K)}, Z_g^{(K)} + \eta^{(K)}) = 0$$

$$g(X_g^{(K)} + \xi^{(K)}, Z_g^{(K)} + \eta^{(K)}) = 0$$

Thus a system of homogeneous equations can be expressed as

$$\xi^{(K)} \cdot f_{X_g} + \eta^{(K)} \cdot f_{Z_g} + f(X_g^{(K)}, Z_g^{(K)}) = 0$$

$$\xi^{(K)} \cdot g_{X_g} + \eta^{(K)} \cdot g_{Z_g} + g(X_g^{(K)}, Z_g^{(K)}) = 0$$

Inserting the initial guesses  $X_g^{(0)}, Z_g^{(0)}$  gives

$$\xi^{(0)} = \frac{g(X_g^{(0)}, Z_g^{(0)}) \cdot f_{Z_g} - f(X_g^{(0)}, Z_g^{(0)}) \cdot g_{Z_g}}{f_{X_g} \cdot g_{Z_g} - f_{Z_g} \cdot g_{X_g}}$$

$$\eta^{(0)} = \frac{f(X_g^{(0)}, Z_g^{(0)}) \cdot g_{X_g} - g(X_g^{(0)}, Z_g^{(0)}) \cdot f_{X_g}}{f_{X_g} \cdot g_{Z_g} - f_{Z_g} \cdot g_{X_g}}$$

The computational scheme in its explicit form can be expressed as

$$\begin{aligned} X_g^{(1)} &= X_g^{(0)} + \xi^{(0)} \\ Z_g^{(1)} &= Z_g^{(0)} + \eta^{(0)} \end{aligned}$$

By inserting  $X_g^{(1)}, Z_g^{(1)}$  into the homogeneous equations again,  $\xi^{(1)}$  and  $\eta^{(1)}$  can be calculated. The iteration is being processed until the absolute values of  $\xi^{(K)}$  and  $\eta^{(K)}$  are less than  $10^{-3}$  then the values of  $X_g$  and  $Z_g$  can be determined.

The values of  $Y_g$  and  $m$  can be calculated as :

$$m = \frac{C_x}{X_g} \quad \text{and} \quad Y_g = \frac{C_y}{C_x} \cdot X_g$$

#### 4. Mechanical hardware

The prototype sensor was made of Dural 79 - TF aluminum alloy. The material has high ultimate tensile strength and low damping. The sensor was machined out of a single block of metal in order to avoid backlash and multi-degree-of-freedom vibration. The platform diameter was chosen as 100 mm with a thickness of 3 mm. This platform design provides sufficient strength to support the largest test piece without deformation and enough rigidity to enable the column to be considered as the only elastic element. The setup is considered as a two degree-of-freedom vibratory system.

The base of the prototype sensor was firmly bolted onto heavy steel plates so that movement of the end of the column is negligible.

#### 5. Electronic hardware

Being accurate, inexpensive, and easily installed, strain gauges were selected as the primary sensing elements. They were mounted on the column and connected into a Wheatstone bridge for signal processing. The output signals from the Wheatstone bridge were amplified by instrumentation amplifiers.

When measuring the natural frequencies of vibration of the system, Fast Fourier Transform (FFT) is employed to convert the amplified signals from time domain to frequency domain so that calculation of frequency is simpler and more accurate.

The signals are fed to a microcomputer via a Data Acquisition Card consisting of analog-to-digital converters and digital-to-analog converters.

Figure 3 shows the arrangement of the signal processing hardware.

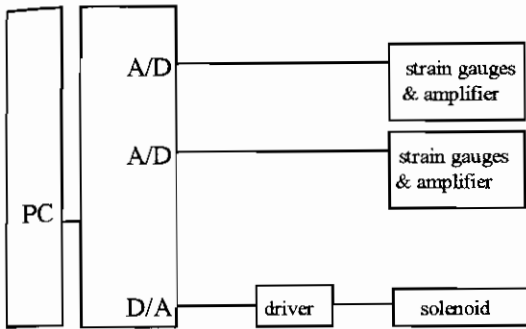


Figure 3. Block diagram of the signal processing hardware

## 6. Software

The sensor is controlled by a program written in C++ which consists of four parts. Part 1 performs static measurement and computation to obtain the values of  $V_x$  and  $V_y$ . Part 2 implements the control function that sends a signal to switch on the solenoid actuated bolt to deliver an impact to the platform which sets the system into free vibration. Parts 3 and 4 carry out the frequency measurement and calculation of the mass and the spatial location of centre of mass of a given part.

## 7. The first stage experiment results: verification for the measurement of $X_g$ , $Y_g$ and $Z_g$

In order to test the feasibility of the sensor, three test pieces of different dimensions were manufactured. The location of the centre of mass of each test piece was determined using the sensor[4].

The calculated coordinates of the centres of mass were compared with the actual values as shown in Table 1 below.

Specimen no.	1	2	3
Mass (g)	463	454	501
Dimension (mm)	∅60 x 40	∅43 x 40	40 x 40 x 40
Material	Aluminum alloy	Mild steel	Mild steel
Actual value of $Z_g$ (mm)	20	20	20
Experimental value of $Z_g$ (mm)	20.39	19.92	19.46
Error in mm	+ 0.39	- 0.08	- 0.34
Error in %	1.987	0.395	2.681

Actual value of $X_g$ (mm)	30	21.5	20
Experimental value of $X_g$ (mm)	29.75	21.7	20.27
Error in mm	- 0.25	+ 0.2	+ 0.27
Error in %	0.833	0.93	1.35

Actual value of $Y_g$ (mm)	30	21.5	20
Experimental value of $Y_g$ (mm)	30.28	21.2	20.28
Error in mm	+ 0.28	- 0.3	+ 0.28
Error in %	0.933	1.395	1.38

Table 1. Comparison of measured and actual locations of centres of mass.

As can be seen from Table 1, the calculated values of  $X_g$ ,  $Y_g$  and  $Z_g$  were all within  $\pm 0.4$  mm of the actual values. This shows that the proposed sensor is capable of measuring, to an accuracy of less than  $\pm 0.4$  mm, the spatial location of the centre of mass of an object placed on the platform.

## 8. Conclusion

The sensor has two features. First, it operates by measuring parameters related to the inertia of the part. Second, it incorporates an inexpensive personal computer.

Three advantages of the sensor are that, unlike vision systems, it is not affected by poor lighting, dust and fumes, it can detect defects such as internal holes which would escape detection by vision-based inspection system, it is also inexpensive compared with vision system.

The accuracy of measurement is affected by the design of the sensor such as the length and cross-sectional dimension of the column as well as the position of the object on the platform relative to the neutral axes of the column.

The second stage of experiment will proceed to measure both the mass and the spatial location of the centre of mass simultaneously. A further development of the sensor is to add intelligence to it so that possible defects of the part can be identified by the system.

## Acknowledgements

The authors would like to express appreciation for the financial support given by the Department of Mechanical Engineering, University of Hong Kong.

## References

For a book citation:

- [ 1 ] Pau L.F., Computer Vision for Electronics Manufacturing. Plenum Press, 1989, Pages 40 and 148.

[ 2 ] Beards C.F., Structural Vibration Analysis. Halsted Press , 1980, John Wiley & Sons.

[ 3 ] Schwarz, H.R., Numerical Analysis. John Wiley & Sons, 1989, Pages 216--221.

For a conference citation:

[ 4 ] SM Tam and KC Cheung, An Inertial Sensor for Parts Inspection. Proceedings of 1995 IEEE International Conference on Robotics and Automation, vol. 1, pp 812-816, May 21-27,1995.